Dynamics of three-dimensional Ising spin glasses in thermal equilibrium

Andrew T. Ogielski
AT&T Bell Laboratories, Murray Hill, New Jersey 07974
(Received 10 July 1985)

I present an analysis of the dynamic behavior of short-range Ising spin glasses observed in stochastic simulations. The time dependence of the order parameter $q(t)=\overline{\langle S_x(0)S_x(t)\rangle}$—which is the same as that of the structure factor—and the time dependence of the related dynamic correlation functions have been recorded with good statistics and very long observation times. The spin-glass model with a symmetric distribution of discrete nearest-neighbor $\pm J$ interactions on a simple-cubic lattice was used. Simulations were performed with a special fast computer, allowing for the first-time investigation of the equilibrium dynamics for a wide range of temperatures ($0.7 \leq kT/J \leq 5.0$) and lattice sizes (8^3, 16^3, 32^3, and 64^3). I have found that the empirical formula $q(t)=ct^{-x}\exp(-\omega t^{\beta})$ with temperature-dependent exponents $x(T)$ and $\beta(T)$ describes the decay very well at all temperatures above the spin-glass transition. In the spin-glass phase, only the algebraic decay $q(t)=ct^{-x}$ could be observed, with different temperature dependences of the exponent $x(T)$. The dynamic scaling hypothesis and finite-size scaling explain well the observed temperature and size dependence of the data, and the functional form of the correlation functions is compatible with the scaling form if corrections to scaling are taken into account. The scaling behavior and the dynamic and static critical exponents found in my simulations are in reasonable agreement with recent experiments performed on insulating spin glasses, showing that despite its simplicity the discrete model of spin glasses analyzed in this work displays behavior similar to that seen in nature.

I. INTRODUCTION

Although slow, nonexponential relaxation has become an important symptom of the "spin-glass syndrome,"[1] our understanding of the dynamics of spin glasses is not quite satisfactory, neither on the experimental nor on the theoretical level. In recent years a number of experiments[2] have been performed and more data on equilibrium dynamics has become available. Nonexponential decay of dynamic correlation functions[3–5] and rapid growth of correlation times as the temperature approaches T_g from above have been clearly established. In the absence of a satisfactory theoretical description, however, the data do not allow one to determine unambiguously the shape of the correlation functions, nor the temperature dependence of correlation times, and quite often several distinct, currently popular fits may describe the results equally well in the reported frequency and temperature range.[6,7] Moreover, in principle there is no reason to expect some universal behavior among all materials called spin glasses, and determination of classes of systems displaying similar dynamics has not yet been achieved.

On the theoretical side, only the dynamics of the infinite-range mean-field theory of spin glasses has been analyzed in some detail,[8,9] predicting exponential decay of correlations and critical slowing down, $\tau \propto (T-T_g)^{-z\nu}$, above T_g with the dynamic exponent $z\nu=2$, and algebraic decay of correlation functions below T_g, with an exponent which decreases with temperature from the value of $\frac{1}{2}$ at T_g. In general, mean-field exponents need not describe real three-dimensional systems, and indeed experimental data do not agree with mean-field-theory predictions. A phenomenological renormalization group was proposed for short-range spin glasses,[10] where scaling of the energy barriers $\tilde{V}$ with the length scale was used to characterize the temperature dependence of the correlation times defined by the Kramers relation $\tau \propto (\tilde{V}/T)$. Such arguments imply; (i) simple Arrhenius behavior at low temperatures for dimensions lower than the lower critical dimension (LCD), i.e., $\tilde{V}$ is roughly constant, (ii) exponential growth $\tau \sim \exp(c/T^3)$ at the LCD, and (iii) the usual critical slowing down above the LCD. Extrapolations from the high-temperature behavior were employed[11,12] to suggest that two-dimensional short-range Ising spin glasses belong to class (i), but a more marginal behavior cannot be excluded.[13,14] Earlier analysis of average correlation times in the three-dimensional model[15] excluded the simple Arrhenius behavior (i), and an attempt to fit the data taken at not too low temperatures to an exponential form (ii) would require that the power of temperature in the exponent be much higher than 3. Of all predictions of phenomenological renormalization only the critical behavior, $\tau \sim (T-T_g)^{-z\nu}$, is consistent with numerical data. Another exponential law, $\tau \sim \exp(c/T^{z\nu})$, with an unspecified exponent $z\nu$ appeared in the content of the so-called zero-temperature transition hypothesis.[16] Both numerical[15,16] and experimental[6] data taken well above $T=0$ were fitted to this form, and indeed this parametrization could be used in this temperature regime with sufficiently high values of $z\nu$, but it appears accidental because the static behavior predicted in Ref. 16 does not agree well with observed low-temperature behavior.

The fluctuation dynamics of spin glasses was also considered separately, without reference to static correlations. Difficulties with the classical Arrhenius law in describing experimental spin-glass data led to the introduction[17] of

the Vogel-Fulcher (VF) law,[18] $\tau \simeq \tau_0 \exp[E_0/(T-T_0)]$. This phenomenological relation has long been known in the literature devoted to viscous fluids and glasses. The meaning of the parameter T_0 is not entirely clear. A comparison of fits to certain experimentally determined characteristic times for various spin glasses above T_g indicates[7] that critical slowing down describes the data better than the VF law. Large deviations from the VF law close to T_g have been reported earlier[19] but no comparison to alternative fits was performed.

More recently, several papers addressed the more general issue of plausible mechanisms of relaxation in random systems, producing various estimates of the asymptotic behavior of dynamic correlation functions. An analysis of dilute Ising ferromagnets[20] based on the concept of isolated rigid clusters of spins was extended to Ising spin glasses.[21] I will discuss predictions of this work later in Sec. V, and only say here that independent cluster models do not seem suitable for the description of three-dimensional spin glasses.

Another class of models designed to explain the dynamics of glassy systems by hierarchical rather than independent parallel relaxation processes has been proposed in Ref. 22, and various types of nonexponential relaxation functions were obtained, including the Kohlrausch function $\exp(-\omega t^{\beta})$, $0<\beta<1$. It is plausible that general scaling ideas contained in that work can be applied to analyze the stochastic dynamics of spin glasses. This brief introduction certainly does not exhaust all ideas and models invoked to explain the puzzling features of spin-glass dynamics; these may be found in references provided in cited papers.

In this report I consider equilibrium dynamics of fluctuations in three-dimensional short-range Ising spin glasses both above and below the transition temperature T_g. Nonequilibrium relaxation far below T_g will not be addressed. I present the results of simulations of a model spin glass with a simple Hamiltonian, controlled distribution of disorder variables and stochastic dynamics, which is presumably adequate for modeling of real physical dynamic processes. The plan of the paper is as follows. In Sec. II, I explain the spin-glass model and its dynamics, which have been implemented in computer simulations. Section III contains some important technical details. In Sec. IV, I provide a short summary of static equilibrium properties of three-dimensional Ising spin glasses recently determined in Monte Carlo simulations. Dynamic correlation functions are analyzed in Sec. V. Various definitions of correlation time are reviewed in Sec. VI, and the temperature dependence of computed spin-glass correlation times is analyzed. Scaling of dynamic correlation functions is discussed in Sec. VII. Finally, in Sec. VIII comparison with recent experiments is performed. Main results are summarized in Sec. IX.

II. ISING SPIN-GLASS MODEL AND ITS DYNAMICS

I will discuss a model of spin glasses defined by the Hamiltonian[23]

$$H=-\sum_{xy} J_{xy}S_xS_y - h\sum_x S_x \tag{1}$$

with Ising spins $S_x=\pm 1$, and with discrete random nearest-neighbor interactions $J_{xy}=\pm J$ distributed independently on bonds of a simple cubic lattice with probability $\frac{1}{2}$ for each value. Periodic boundary conditions are used throughout, and the magnetic field h is held equal to zero. It is noted that although simple, this model contains the essential features of spin glasses: randomness and frustration.[24] Moreover, restriction to discrete J_{xy} should not seriously limit the generality of results at finite temperatures, because the spin-glass correlation length ξ diverges at a finite temperature $k_BT_g/J\sim 1.15$—1.20 in this model.[15,25] (T_g has been determined by a variety of methods and the result always lies in this interval; now it seems that the best choice is $k_BT_g/J=1.17$—1.18.)

Monte Carlo simulation—essentially the only established method currently available for investigation of statistical properties of the model (1)—is intrinsically dynamical in nature. The simulation is an ergodic, irreducible Markov process with homogeneous discrete time evolution. A single time step corresponds to one attempt to change the state of a single spin, and the evolution of the system is described by the master equation (which despite its name is merely a restatement of the Markovian property)

$$\begin{aligned} &P(\sigma,t+1)=\sum_{\sigma'} W(\sigma\,|\,\sigma')P(\sigma',t)\ , \\ &P(\sigma,t=0)=P_0(\sigma) \end{aligned} \tag{2}$$

for the probability distribution $P(\sigma,t)$ defined on the phase space, i.e., space of all states $\sigma=\{S_x\}$. If evolution of a single state is of interest, we put $P_0(\sigma)=\delta(\sigma,\sigma_0)$. The transition-matrix element $W(\sigma'\,|\,\sigma)$ represents the conditional probability of state σ going into state σ' in a single time step. I used the single-spin-flip heat-bath Monte Carlo method, where $W(\sigma'\,|\,\sigma)=0$ unless states σ,σ' differ by no more than one spin, and the probability of a single-spin change $S_x\rightarrow S_x'$ depends only on the current value of a local field acting on S_x, and not on S_x itself,

$$\begin{aligned} &\mathrm{Prob}(S_x'=+1)=e^{f_x}/(e^{f_x}+e^{-f_x})\ , \\ &f_x=\frac{1}{T}\left[\sum_y J_{xy}S_y+h\right]\ . \end{aligned} \tag{3}$$

With such transition probabilities the detailed balance condition is satisfied, and for any initial distribution $P_0(\sigma)$ the "running" distribution $P(\sigma,t)$ converges to the equilibrium Boltzmann distribution as $t\rightarrow\infty$.

The time unit used in this paper, Monte Carlo step per spin (MCS), corresponds to a time in which *each* spin was given one chance to change its state. This unit aggregates some 10^3—10^5 spin-spin updates for lattice sizes discussed here, which justifies the use of continuous time variable in analysis of the data.

In order to characterize the dynamics of equilibrium thermal fluctuations I will analyze the average properties of trajectories in phase space, with initial states distributed according to Boltzmann distribution and evolving according to (2). This is achieved through the study of dynamic correlation functions. The average spin-spin correlations

$$G(x-y,t)=\overline{\langle S_x(0)S_y(t)\rangle}$$
$$=\int dq\, e^{iq(x-y)}\int dt\, e^{-i\omega t}S(q,\omega) \quad (4)$$

are particularly important. Here an explanation of notation is in order. Throughout this paper the angular brackets represent averages over the ensemble of trajectories in thermal equilibrium when used for time-dependent quantities, or static equilibrium averages when used for time-independent quantities. In both cases the bar denotes configurational averaging over all random bond realizations, and/or spatial averaging over one sample, whichever is appropriate. This averaging is essential, because, in general, the nonaveraged correlations $\langle S_x(0)S_y(t)\rangle$ for distinct pairs of sites x,y (but with fixed separation $x-y$) will have a broad range of values, reflecting the inhomogeneity of the lattice and lack of translation invariance. This simple observation has several important consequences for spin glasses with *symmetric* distributions of ferromagnetic and antiferromagnetic interactions J_{xy}.

(1) The distribution of values of $\langle S_x(0)S_y(t)\rangle$ for distinct spin pairs and with $r=x-y$ and time t fixed is also symmetric, giving upon averaging over disorder

$$\overline{\langle S_x(0)S_y(t)\rangle}=\delta_{xy}\overline{\langle S_x(0)S_x(t)\rangle}\ . \quad (5)$$

In other words, the structure factor $S(q,\omega)$ is independent of momentum transfer q. This has been seen experimentally in materials with negligible residual short-range order,[26] and indeed should be a criterion for experimental characterization of "good" maximally frustrated spin glasses.

(2) As a consequence, the equilibrium (dc) susceptibility must follow the Curie law

$$T\chi=\frac{1}{V}\sum_{xy}\overline{\langle S_xS_y\rangle}=1\ . \quad (6)$$

Such behavior was observed in my simulations.

(3) According to (5), it is sufficient to consider the function

$$q(t)=\overline{\langle S_x(0)S_x(t)\rangle}=\frac{1}{V}\sum_{x}\overline{\langle S_x(0)S_x(t)\rangle}\ . \quad (7)$$

It has been employed by Edwards and Anderson[23] to define the spin-glass order parameter q *without the notion of the ordering field:*

$$q=\lim_{t\to\infty}\lim_{V\to\infty}\overline{\langle S_x(0)S_x(t)\rangle} \quad (8)$$

and ever since has played the central role in development of theoretical ideas about spin glasses.

It is worthwhile to make a digression on the geometric interpretation of $q(t)$: it is a measure of the average distance traveled by the system in the phase space in time t. Such metric construction is particularly appealing for Ising spins, and indeed has been very successful in the development of the mean-field theory of spin glasses.[27] If we define the "overlap" q_{12} of two states $\sigma_1=\{S_x^{(1)}\}$ and $\sigma_2=\{S_x^{(2)}\}$,

$$q_{12}=\sum_x S_x^{(1)}S_x^{(2)}=N_{\uparrow\uparrow}-N_{\uparrow\downarrow}\ , \quad (9)$$

where $N_{\uparrow\uparrow}(N_{\uparrow\downarrow})$ denotes the number of spins having the same (opposite) orientation in both states, than the function $d(\sigma_1,\sigma_2)=N_{\uparrow\downarrow}$ has all properties of a metric defining the distance on the phase space. A related geometrical realization of the phase space can be given: If the states σ are identified with corners of a hypercube in a V-dimensional space, the metric $d(\sigma_1,\sigma_2)$ is equal to the minimal number of edges connecting corners σ_1 and σ_2. Such a model of phase space may be useful to visualize the time evolution of a state as a random walk on a V-dimensional unit hypercube, and also establishes a relationship with Shannon's information theory:[28] If Ising spins are given values of 0,1 rather than ±1, $d(\sigma_1,\sigma_2)$ becomes the Hamming distance, various dynamically defined entropies and dimensions can be employed to characterize the time evolution, etc.

Another useful correlation function which is studied characterizes the fluctuations of the order parameter $q(t)$ around its average value, and in this sense plays the role of the order-parameter correlation function. It is the time-dependent nonlinear susceptibility

$$\chi_{\rm SG}(t)=\frac{1}{V}\overline{\left\langle\left[\sum_x S_x(0)S_x(t)\right]^2\right\rangle} \quad (10)$$

which has been so named because it converges asymptotically to the usual static nonlinear susceptibility[29]

$$\chi_{\rm SG}(t)=\frac{1}{V}\sum_{xy}\overline{\langle S_x(0)S_y(0)S_x(t)S_y(t)\rangle}$$
$$\underset{t\to\infty}{\to}\frac{1}{V}\sum_{xy}\overline{\langle S_xS_y\rangle^2}=\chi_{\rm SG}\ . \quad (11)$$

For finite systems the order parameter $q(t)$ cannot be used to detect any long-range spin-glass ordering [cf. (8)], because it always decays to zero. It is advantageous to test the rigidity of low-temperature states with another correlation function

$$\overline{\langle\,|q(t)|\,\rangle}=\left\langle\left|\frac{1}{V}\sum_x S_x(0)S_x(t)\right|\right\rangle\ . \quad (12)$$

If there is long-range order (in the $V\to\infty$ limit), then for finite systems the statistically significant equilibrium states should have large overlaps of both signs, and while $q(t)$ will average virtually to zero at very long times, its average absolute value will decay to a size-dependent limit $Q=\langle\,|q(\infty)|\,\rangle$. The existence of long-range spin-glass order will be signaled by convergence of Q to a nonzero value with increasing lattice size, and conversely Q will scale to zero at temperatures at which no long-range order exists. The quantity $\tilde{Q}=(1/V)\chi_{\rm SG}$ could be used equally well for this purpose.

Dynamic correlation functions (7), (10), and (12) recorded in my simulations will be analyzed in the following sections. First, however, the static and dynamic behavior of the three-dimensional Ising spin glasses observed in recent simulations will be reviewed and updated. Further, I will briefly describe some technical details of the compu-

tations, which may be useful for critical evaluation of results and for comparison with related work.

III. RESULTS: STATIC AND DYNAMIC BEHAVIOR

Dynamics of fluctuations should be discussed in the context of static equilibrium behavior. As everywhere else in this work I consider only the case of zero external magnetic field, i.e., temperature T is the only thermodynamic variable controlling the behavior of the system. This section is based on results of recent Monte Carlo simulations.[15,25] These results are extended and updated by inclusion of new numerical data.[30,31]

The behavior of the model (1) of spin glasses can be described as follows. One can identify three distinct temperatures, $T_c = 4.511\ldots$, $T_p \approx 1.80$, and $T_g \approx 1.175$ separating the regions with different static and dynamic behavior (Fig. 1). First, at temperatures higher than the Curie point T_c of the nonrandom ferromagnetic Ising model the simple paramagnetic behavior is observed, and the relaxation functions display the exponential decay law. As the temperature is lowered below T_c, a new type of behavior is observed in the interval extending roughly to temperature $T_p \approx 1.80$ which is marked by a broad maximum of the specific heat C_v, shown in Fig. 2. In this interval the effects of inhomogeneous lattice, which can be characterized by local fluctuations in the density of frustrated plaquetts (and possibly can be related to the so-called Griffiths singularities[32]) already influence the behavior of the system, and are most easily seen in the nonexponential asymptotic decay of relaxation functions. However, in this regime the static spin-glass correlation length as well as correlation times are very small, and increase only very slowly as temperature is decreased. The temperature region around the specific-heat maximum marks the onset of the dramatic growth of correlation times, as well as rapid growth of correlation length ξ and nonlinear susceptibility χ_{SG} as temperature is decreased. The divergence of correlation time—which will be discussed in Sec. IV—is displayed in Fig. 3. These divergences are very well described by scaling and power laws, with the spin-glass transition temperature in the range 1.15—1.20; current best power-law fits as well as best finite-size scaling plots (i.e., with minimal scatter of points, and without corrections to scaling) suggest the

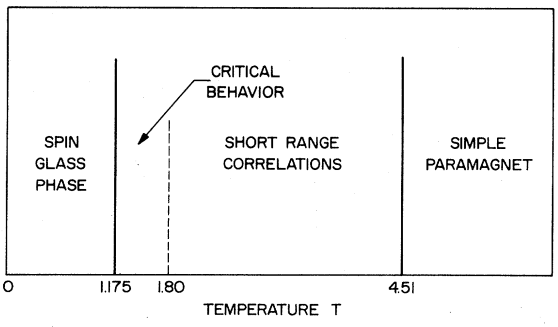

FIG. 1. Graphical representation of distinct temperature regimes observed in the three-dimensional Ising spin glass.

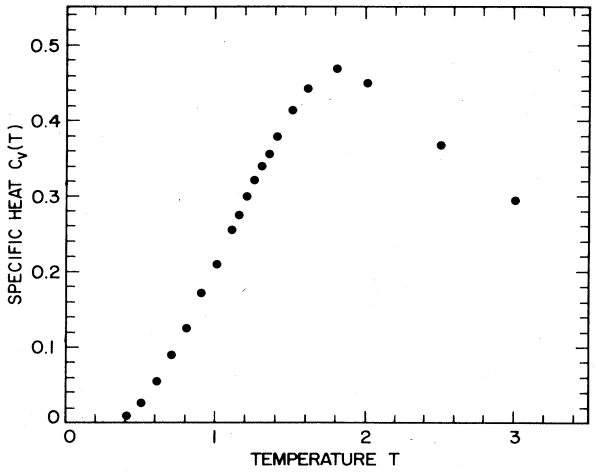

FIG. 2. Temperature dependence of the specific heat C_v.

midpoint value $T_g = 1.175 \pm 0.025$. With this choice of T_g the fits and finite-size scaling (the latter, in principle, can give better exponent estimates) give the following values for the critical exponents: $\nu = 1.3 \pm 0.1$, $\eta = -0.22 \pm 0.05$, $\gamma = 2.9 \pm 0.3$ and from scaling relations $\alpha = -1.9 \pm 0.3$. Error estimates for the critical exponents reflect the uncertainty of the exact location of T_g rather than statistical scatter of the data. Finite-size scaling of the static nonlinear susceptibility χ_{SG}, from which the exponents η and γ are derived, is illustrated in Fig. 4. If the exponent β can be defined (see below), this would give $\beta \approx 0.5$. In fact, since only leading divergences are considered, these numbers should be more correctly referred to as effective exponents. The value of the dynamic exponent z is connected to definition of correlation time, and will be discussed in Sec. VI.

The region below T_g is called the spin-glass phase. Much less is known about thermodynamic properties of

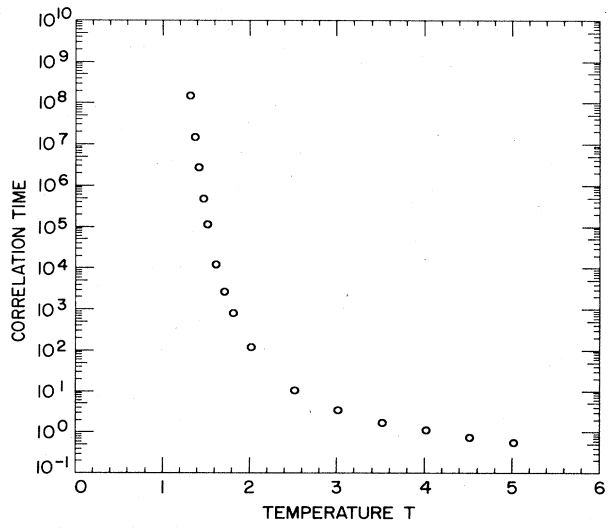

FIG. 3. Temperature dependence of the correlation time τ, defined by Eq. (21).

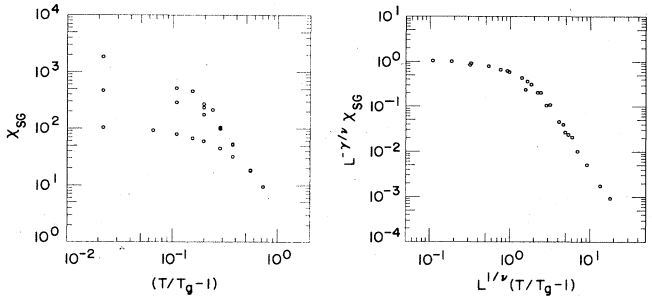

FIG. 4. Static nonlinear susceptibility χ_{SG} for lattices of size 8^3, 16^3, 32^3, and 64^3 (left) is plotted in the scaling form (right). The parameters are $T_g=1.175$, $\nu=1.3$, and $\gamma=2.9$.

this phase, since most of the knowledge is based on the finite-size-scaling analysis done for rather small lattice sizes, and for sizes $L \geq 16$ only at temperatures not lower than $T=1.0$. The reason for these difficulties is that the quantities used for scaling are obtained as asymptotic time limits of various dynamic correlation functions [as in Eq. (11)], and relaxation becomes unbearably slow below T_g. So far, finite-size-scaling results[25,31] limited to a narrow temperature region below T_g are consistent with the hypothesis[25] that the spin-glass phase may be always critical, i.e., characterized by vanishing static order parameter, yet with infinite correlation length and infinite correlation time. Such states should display algebraic decay of static and dynamic correlations. There is not enough evidence for the algebraic decay of static correlations; in fact, in some bond realizations of 32^3 lattices the low-temperature state appeared to be more "rigid," as previously reported.[15]

Much greater lattice sizes and lower temperatures are required to clarify this point. For times up to about 10^8 MCS, however, the decay of dynamic correlations appears to be algebraic in the spin-glass phase.

It should be stressed that dynamics of the spin-glass phase is very different from the behavior of ordinary nonrandom systems in the ordered low-temperature state. There one has two time scales for $T<T_c$ and $\xi \ll L$, one independent of L, and the other diverging as $L \to \infty$ (what corresponds to diverging energy barriers between distinct pure ordered states). The spin-glass phase is different: One cannot make such a separation and the situation is better characterized by the notion of "continuum of time scales." Separation into "fast" and "slow" degrees of freedom seems to be arbitrary and meaningless, and in finite systems the time scales where relaxation functions have values already appropriate for the infinite-volume limit smoothly roll over into faster decay due to finite size.

IV. TECHNICAL DETAILS

Computations were performed with a fast special purpose computer designed and built at AT&T Bell Laboratories by J. H. Condon and the author specially for simulations of various random spin systems. Description of this machine can be found elsewhere.[33]

Correlation functions $q(t)$, $\chi_{SG}(t)$, $\langle |q(t)| \rangle$, and also some others, not discussed here, were recorded for lattices of sizes 8^3, 16^3, 32^3, and 64^3. Since local fluctuations of frustration density in random bond realizations are responsible for the shape of averaged correlation functions, the data analyzed here were recorded for *at least* 64 distinct 8^3 lattices, 32 distinct 16^3 lattices, two distinct 32^3 lattices, and one 64^3 lattice. At higher temperatures more realizations were often used, but at low temperatures the extremely slow relaxation rate made it virtually impossible to include more realizations in configurational averaging. It is believed, and supported by error estimates, that increase of the number of samples would not change significantly the estimated average correlation functions, but a chance of systematic deviations can be excluded only with probabilistic arguments and not rigorously. Nevertheless, with such range of lattice sizes it has been possible to establish for each lattice size L ($V=L^3$) the lowest temperature and the longest time down to which the averaged correlation functions do not differ from analogous function recorded on samples of larger size by more than statistical errors, and thus are not expected to differ from the limiting infinite-volume form.

The other technical points which deserve attention are recording of time correlations for individual bond realization prior to configurational averaging, and assuring that measurements are performed in thermal equilibrium. First, since successive measurements of overlaps

$$(1/V)\sum_x S_x(0)S_x(t)$$

and other quantities along a single trajectory evolving from the state $\{S_x(0)\}$ are taken at intervals shorter than the "longest time scale," the consecutive data points are strongly correlated, also at very long times. (Here the longest time scale is determined in a heuristic manner as the range of times in which single overlaps begin to assume negative values and fluctuate around zero, as shown in Fig. 5.) This requires that averaging must be done over

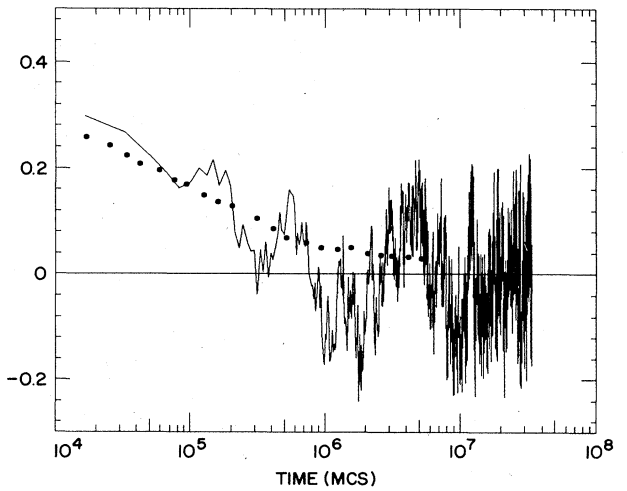

FIG. 5. Tail of a single trajectory $(1/V)\sum_x S_x(0)S_x(t)$, for $T=1.35$ and a 32^3 lattice. The "longest time scale" is heuristically determined as the decade of time in which the overlaps begin to fluctuate around zero. Dots represent $q(t)$ averaged over 170 trajectories.

many statistically independent trajectories, originating from initial states drawn independently from the equilibrium Boltzmann distribution. Second, care has been taken to assure that measurements have been performed in thermal equilibrium, which is a nontrivial problem for this slowly relaxing system. The entropy factor, rather than the energy value, is essential for correct thermodynamic averaging, because of very high degeneracy of energy levels. The required Boltzmann distribution of initial states was obtained as follows. Slow cooling to low temperatures at which measurements were done was performed with small temperature decrements ($\Delta T=0.01$–0.05), and after each change the system was allowed to relax to equilibrium over a time longer than the longest time scale determined at the previous temperature stop. Once the equilibrium state was established at the required temperature, the measurements were performed over a time often several orders of magnitude longer than the time in which $q(t)$ decays virtually to zero. A collection of independent equilibrium states was saved and stored at each temperature, and thus successive cooling and measurement cycles could be initialized with already relaxed configurations, rather than beginning again at high temperatures.

Obviously, for each lattice size a value of low temperature was finally reached at which the relaxation became so slow that complete correlation functions could no longer be recorded. At this point measurements were discontinued. An exception was made for the short- and intermediate-time measurements for 32^3 lattices below $T=1.10$, since the comparison with results obtained in fully relaxed 16^3 lattices showed that the functional form of correlation functions and these temperatures and in these time regimes is not visibly modified by possible nonequilibrium effects.

V. THE SHAPE OF DYNAMIC CORRELATION FUNCTIONS

Time dependence of dynamic correlation functions $q(t)$ and $\chi_{SG}(t)$ at different temperatures is discussed in this section. The averaging of correlation functions over sufficiently many random bond realizations has been performed to obtain reproducible results. For each individual bond realization averaging has been done over many statistically independent trajectories. Typically between 20 and 500 initial states were taken depending upon lattice size and time range studied. The variation among single trajectories is strongly damped by spatial averaging included in definitions (7) and (10), when dynamic fluctuations occur on length scales much shorter than the lattice size; however, at long times were fluctuations are due to correlated processes occurring on longest length scales present at a given temperature, much averaging has to be done to obtain smooth time dependence of correlation functions, as can be readily seen from Fig. 5.

The autocorrelation functions $q(t)$ at temperatures above T_g and lattice size 64^3 are shown in Figs. 6 and 7. All recorded data points are shown together with statistical error bars. Continuous lines correspond to fits described later in this section. At short times and at higher temperatures the errors are smaller than the

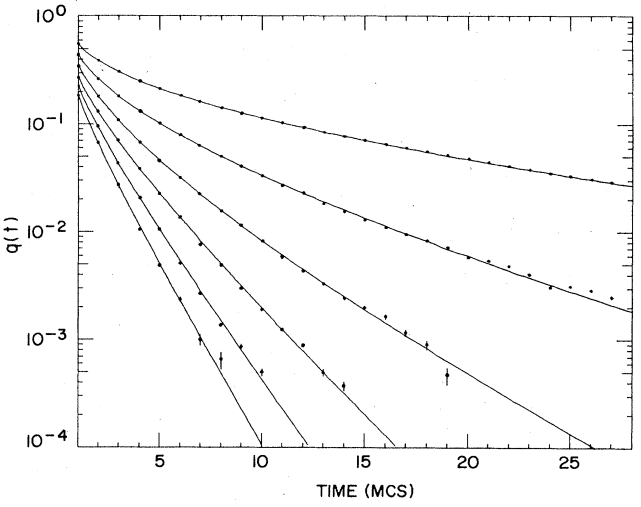

FIG. 6. Dynamic correlation functions $q(t)$ at high temperatures. From bottom to top, $T=5.0$, 4.5, 4.0, 3.5, 3.0, and 2.0. Error bars are shown unless smaller than point size. Continuous lines are fits described in the text. Lattice size 64^3.

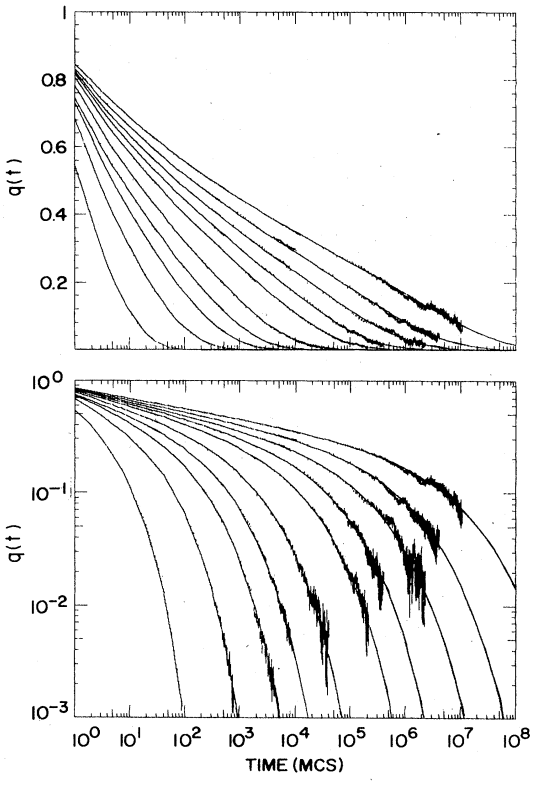

FIG. 7. Dynamic correlation functions $q(t)$ above T_g. Short-time behavior is well seen in the semilogarithmic plot (top), long-time behavior can be seen only in the log-log plot (bottom). Data points are shown together with error bars. From left to right, the temperatures are $T=2.50$, 2.00, 1.80, 1.70, 1.60, 1.50, 1.45, 1.40, 1.35, and 1.30. Lattice size 64^3.

linewidth. Comparison with analogous sets of functions recorded for smaller lattice sizes (performed like that in Fig. 9) has shown that for temperatures $T > 1.30$ the data in Figs. 6 and 7 are not influenced by finite-size effects, i.e., the shape of correlation functions is the same as for the infinite-volume limit. This observation is additionally supported by the observation that the correlation length is not greater than about 15 lattice spacings at the lowest temperature displayed ($T=1.30$).

Time dependence of $q(t)$ around, and below T_g is shown in Fig. 8, this time for lattice size 32^3. For temperatures below $T=1.10$ the decay has not been followed until $q(t)$ essentially decays to zero (within errors) as it has been done for higher temperatures, because even for this finite lattice and my fast computer this would require an astronomical computing time. Smaller lattices, however, still relax completely below T_g, i.e., negative contributions to $q(t)$ are frequently recorded. This finite-size effect is shown in Fig. 9, when I compare the correlation functions $q(t)$ at fixed temperature and time as the lattice size changes. I conclude that the plots of $q(t)$ shown in Fig. 8 are *not* influenced by finite-size effects for $T < T_g$, while finite size clearly speeds up the relaxation at long times in plots corresponding to temperatures little above T_g ($T=1.30$, 1.25, 1.20 in Fig. 8).

A look at the log-log plots of $q(t)$ shown in Figs. 7 and 8 tells us that as temperature is decreased the longer part of the decay can be very well approximated by straight lines. This is a sign of developing scale-invariant fluctuations reflected in the power-law decay of correlation functions. Also, another important information is contained in Figs. 8 and 9. One cannot identify any simple description of fluctuations at low temperatures in terms of well-separated "fast" and "slow" time scales as some authors suggested: One sees a continuum of time scales building up the algebraic decay law, and the influence of finite size

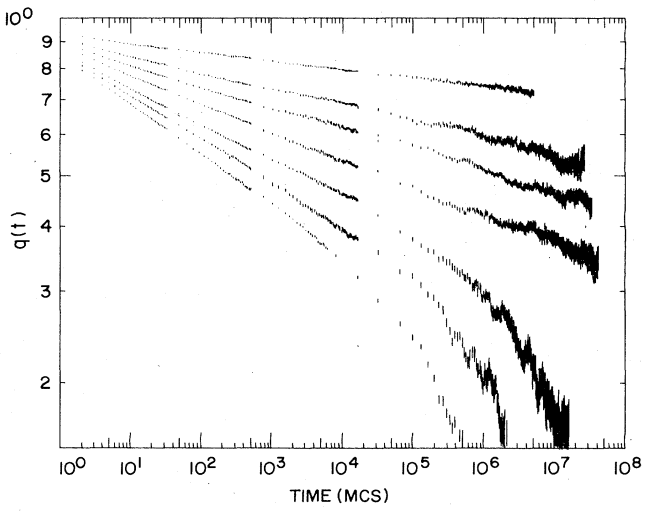

FIG. 8. Dynamic correlation functions $q(t)$ for temperatures around and below T_g. Data are shown together with error bars. Temperatures $T=1.30$, 1.25, 1.20, 1.10, 1.00, 0.90, and 0.70 (from bottom to top). Lattice size 32^3.

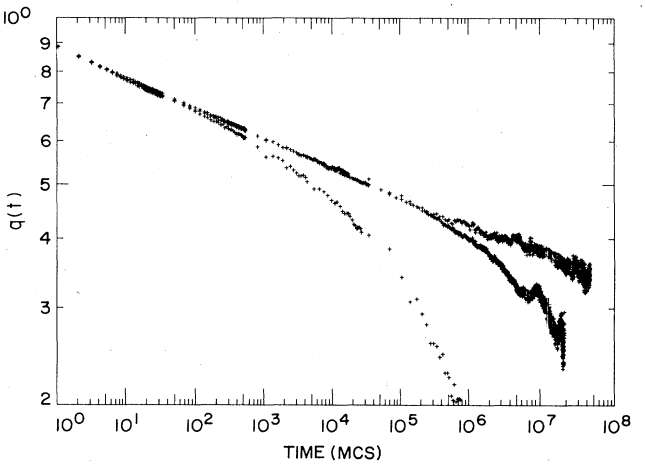

FIG. 9. Effect of finite-lattice size on relaxation below the transition temperature T_g. Data for $T=1.10$ and lattice sizes 8^3, 16^3, and 32^3 are shown: it is seen that for a 16^3 lattice (middle plot) relaxation is not affected by finite size for times $t < 10^6$ MCS, and relaxation in 32^3 lattices (top) is not likely to be affected for all times shown ($t < 10^8$ MCS). Relaxation of smaller lattices of size 8^3 is considerably faster and thus strongly influenced by finite size.

does not appear as an easily identifiable L-dependent long-time scale reflecting the energy barriers between distinct ordered states, but rather a smooth rollover of the algebraic decay into a faster decay induced by a finite-size cutoff is seen at longer times.

Let us now return to the long-time tails of $q(t)$ at $T > T_g$, shown in Figs. 6 and 7. In order to see if at asymptotic times $q(t)$ decays exponentially—and to get a hint at possible alternative nonexponential decay laws—it is advantageous to display the ratio $\tau(t) = -t/\ln q(t)$ versus time t in a doubly logarithmic plot, because for (asymptotically) exponential decay such curves would appear as (asymptotically) horizontal straight lines. Note that the standard way of looking into exponential decay—plots of $\ln q(t)$ versus time—is not good here, because such a method effectively displays only one decade of data.

The plots of $-t/\ln q(t)$ versus t are shown in Fig. 10. The lines of data points clearly do not bend and do not flatten out at all. The straight lines seen in Fig. 10 not only show that the decay is never exponential, they clearly indicate that at longer times the function $\tau(t) = -t/\ln q(t)$ is well described by a fractional power of t, $t^{1-\beta}$ with $0 < \beta < 1$, and that exponent β slowly decreases with temperature.

It is a simple matter now to combine the scale-invariant decay observed at shorter times with the asymptotic Kohlrausch behavior, and to propose the empirical formula

$$q(t) = c\frac{e^{-\omega t^{\beta}}}{t^{x}} . \tag{13}$$

Here all four parameters c, x, ω, and β may depend on temperature. The data points for correlation functions

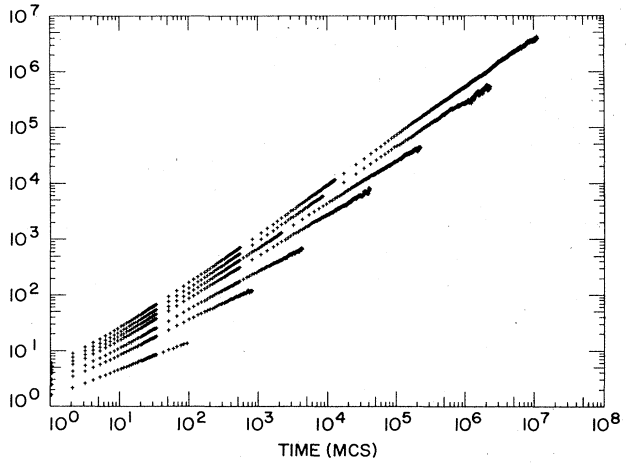

FIG. 10. Correlation functions $q(t)$ shown before in Fig. 7 are converted into a plot of $-t/\ln q(t)$ vs t on the log-log scale. Data points would appear as horizontal lines if $q(t)\sim\exp(-t/\tau)$; this is not seen here. Asymptotically straight lines seen in the graph indicate the Kohlrausch behavior $\exp(-\omega t^{\beta})$ instead, with $\beta<1$. The temperatures are $t=2.50$ (bottom), 2.00, 1.80, 1.60, 1.50, 1.40, and 1.30 (top).

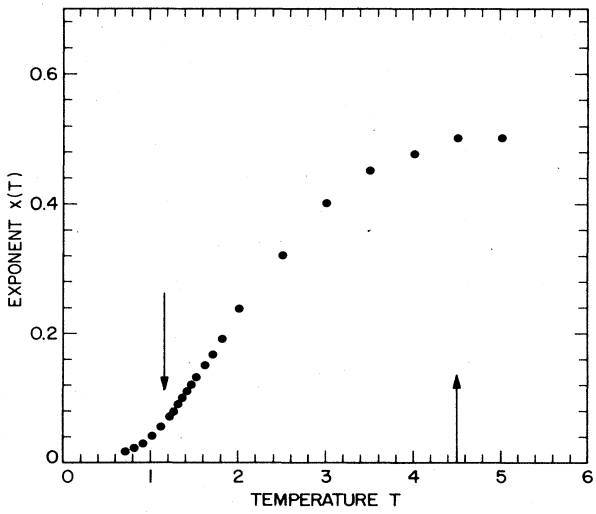

FIG. 12. Temperature dependence of the exponent x defined by Eq. (13) above T_g, and determined from the algebraic decay of $q(t)$ around and below T_g. The arrows mark T_g and T_c as in Fig. 11.

$q(t)$ at each value of the temperature in the range $1.30\leq T\leq 5.0$, were carefully fitted to the function (13) using the weighted nonlinear least-squares method. The best fits are shown together with the data in Figs. 6 and 7. The fits are excellent, and as can be seen they hold tightly both at short and at long times. In the limit of $t\to 0$ the fitting function (13) should be modified in order to satisfy the normalization $q(0)=1$, but this is not essential and it can be seen that (13) describes the data very well even for times of order 1 MCS. Time scales shorter than 1 MCS are of no interest here. Below T_g, i.e., for $T\leq 1.10$, the correlation functions shown in Fig. 8 were fitted to the power law $q(t)=ct^{-x}$.

Temperature dependence of exponents $\beta(T)$ and $x(T)$ is presented in Figs. 11 and 12. Several features are worth stressing. First, as temperature approaches $T_c=4.511\ldots$ (the Curie point of the nonrandom Ising model) from below, exponent $\beta(T)$ tends to a constant value $\beta=1$, i.e., as expected usual exponential decay is seen above T_c. Second, both exponents change linearly with temperature T [or with $(T-T_g)$] in a very good approximation as temperature approaches T_g from above. Third, a change in the temperature dependence of exponents $x(T)$ is seen below T_g.

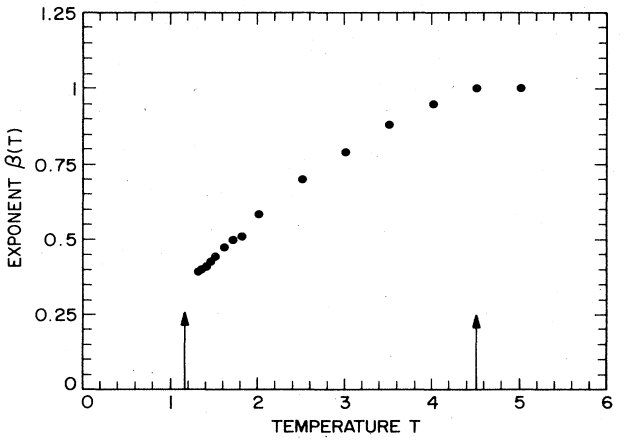

FIG. 11. Temperature dependence of the exponent β defined in Eq. (13). The arrows mark the spin-glass transition temperature T_g and the Curie point T_c of nonrandom Ising model.

Discussion of the shape of correlation functions $q(t)$ presented so far in this section can be repeated *mutatis mutandis* for the normalized time-dependent nonlinear susceptibility,

$$[\chi_{SG}(t)-\chi_{SG}(t=\infty)]/[V-\chi_{SG}(t=\infty)]\ .$$

Normalization is necessary in order to compare different lattice sizes, because $\chi_{SG}(0)=V$. Normalized data have been also fitted to functional form (13) above T_g with very good results, the only obvious difference is that at each temperature the corresponding exponent $x(T)$ is twice as large as the exponent for $q(t)$ (cf. Fig. 17). One set of $\chi_{SG}(t)$ data is shown for illustrative purposes in Fig. 13, where asymptotic decay to a constant value χ_{SG}, assumed in Eq. (11), is easy to see. In fact, nonlinear susceptibilities determined in this manner for distinct lattice sizes were used to find finite-size-scaling functions and static critical exponents.

Time dependence of the averaged absolute value of overlaps $\overline{\langle|q(t)|\rangle}$ defined by Eq. (12) looks similar to that of $\chi_{SG}(t)$, and the asymptotic value $Q=\langle|q(\infty)|\rangle$ can be easily determined. One or two decades of time are required in the asymptotic region to ascertain that there is no further decay. The values of Q for different lattice sizes are plotted in Fig. 14. As expected, at higher temperatures the "order parameter" Q scales quickly to zero with increasing lattice size. However, in the narrow range

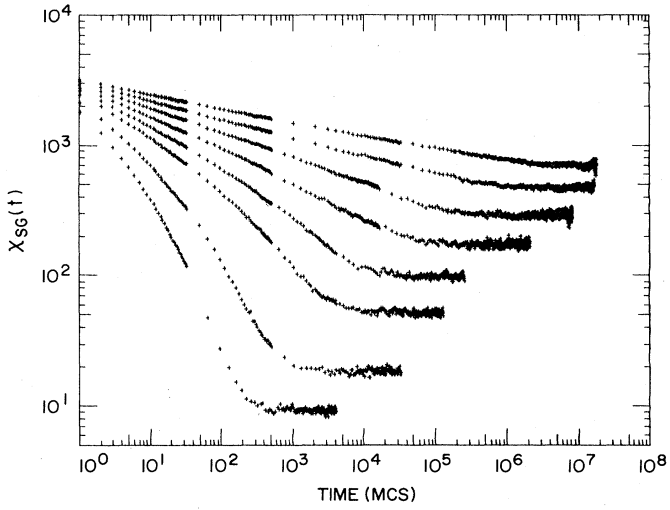

FIG. 13. Decay of the dynamic nonlinear susceptibility $\chi_{SG}(t)$ with time. Data points averaged over 32 distinct lattices of size 16^3, for temperatures $T=2.0$ (bottom), 1.8, 1.6, 1.5, 1.4, 1.3, 1.2, and 1.1 (top).

of temperatures below T_g one does not see a rapid convergence of Q to a nonzero limit, which is expected to happen in ordinary transitions to an ordered state. The issue of the existence of a genuine long-range order below T_g would be resolved if low-temperature data were available for larger lattice sizes, this is not possible at present. Data shown in Fig. 14 are consistent with the hypothesis that spin-glass phase remains in the critical state below T_g.

Further analysis of the dynamic correlation functions in the framework of dynamic scaling theory[34] will be presented in Sec. VII. Below, several qualitative observations on the nature of relaxation processes will be provided.

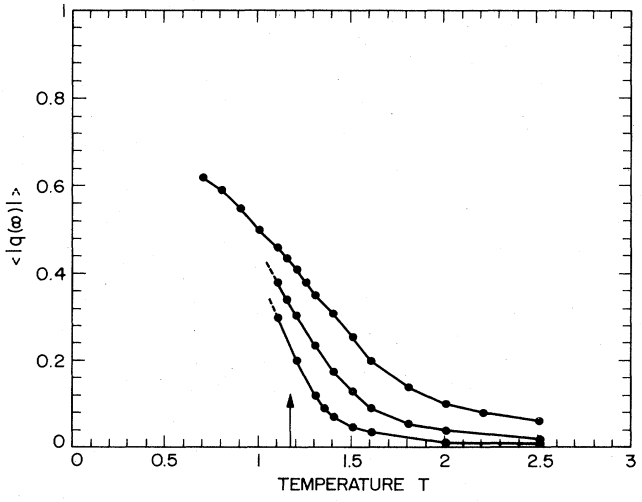

FIG. 14. Temperature dependence of the "order parameter" $\langle |q(\infty)| \rangle$ for lattice sizes $L=8$ (top curve), 16, and 32 (bottom curve). The lines are guides for the eye only. The arrow marks spin-glass transition temperature T_g.

The information gathered during recording of correlation functions for individual bond realizations (before configurational averaging) can be used for a tentative explanation how the long-time Kohlrausch behavior $\exp(-\omega t^{\beta})$ arises from averaging over fluctuations. It appears that in the $d=3$ spin-glass case this form is due to averaging over approximately independent relaxation processes occurring "in parallel" in different geometric environments in the random lattice. For each fixed, small region the asymptotic behavior of locally defined "$q(t)$" is different, and not necessarily of form (13), only after averaging over all distinct local bond configurations the form (13) is obtained. The functional form of the averaged correlation function is reproducible: even when different lattice sizes are compared at temperatures where the correlation length is much shorter than the lattice sizes, and finite-size effects cannot be seen, the same shape is observed once the averaging over sufficiently many bond realizations has been performed.

A more direct demonstration that the long-time Kohlrausch behavior arises from averaging over independent fluctuating regions of the lattice has been achieved as follows. I have recorded with high precision the correlation functions independently on 32 distinct lattices of size 16^3 at $T=2.00$; at this temperature the nonexponential decay is clearly seen, but correlation length ξ is of the order of few lattice lattice spacings. All individually recorded functions $q(t)$ are plotted together in Fig. 15(a) for logarithmically spaced values of time. While only a very small spread of values is seen for short times, differences among distinct bond realizations produce a substantial scatter of values of $q(t)$ at longer times. Nevertheless, after averaging these individual functions $q(t)$ one obtains a smooth Kohlrausch function, exactly the same as recorded for other sizes, and in particular the same as that fitted to data recorded on a 64^3 lattice. This effect of configurational averaging is demonstrated in Fig. 15(b).

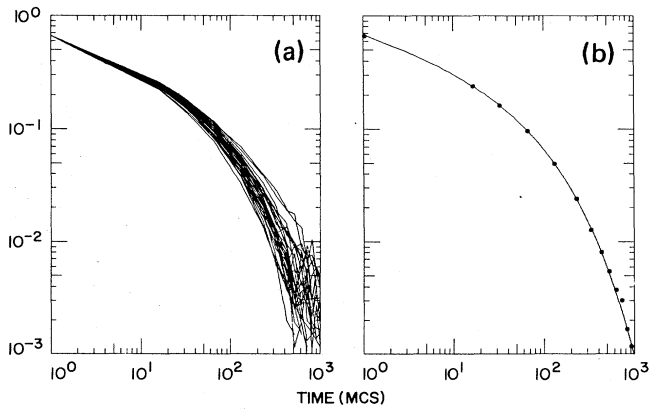

FIG. 15. (a) Correlation functions $q(t)$ recorded for 32 distinct 16^3 lattices at $T=2.00$. Logarithmically spaced data points are connected by straight-line segments. Each curve represents the average over 512 trajectories. Substantial fan-out of values at long times is seen. (b) The circles correspond to data of (a) averaged over bond realizations. They are superimposed on the fit to $q(t)$ recorded for size 64^3, shown in Fig. 7.

It can also be seen that the long-time behavior of the relaxation functions above T_g does not result from averaging over the contributions of independently relaxing, virtually decoupled "rigid unfrustrated compact clusters," as was proposed in Ref. 21. The asymptotic exponential logarithmic behavior, $q(t) \sim A \exp[-B(\ln t)^{3/2}]$ proposed by these authors does not match *any* part of the long-time tails of observed correlation functions shown in Figs. 6 and 7. (Of course, one does not expect this function to approximate the data at shorter times.) Disagreement with predictions of Ref. 21 indicates that the approximation of the $d=3$ spin-glass model at higher temperature (but lower than the Curie point T_c of the pure system) by a collection of independent, "rigid" unfrustrated clusters of tightly coupled spins is not suitable, and does not describe well the processes which actually take place.

I have also examined directly the local spin-spin correlation functions $\langle S_x S_{x'} \rangle$ for all pairs of sites x,x' and different separations $x-x'$ in order to see how spin correlations $\langle S_x S_{x'} \rangle$ are correlated with random lattices on which they "live." This was done for a couple of 32^3 lattices and a wide range of temperatures. Although the distribution of values of local correlations at a fixed distance and temperature is very broad, this analysis did not show any obvious candidates for strongly correlated compact clusters of spins which would be only weakly coupled to the rest of the lattice. An extended account of the investigation of "geometry of spin-glass ordering" will be presented in a separate publication.

VI. THE CORRELATION TIMES

In this section the temperature dependence of dynamic correlations will be examined. First, however, the very notion of the correlation time will be reviewed. The definition of the correlation time, just like the definition of the (static) correlation length ξ, is not unique. Various definitions of the latter were elegantly discussed in Ref. 35, where the notions of the "true correlation range" and "effective correlation range" were compared, as well as other definitions of ξ based on different moments of the spatial correlation function of the local order parameter were introduced. The situation with dynamic correlations is similar.

Using a continuous (rather than discrete) time version of the master equation

$$\frac{\partial}{\partial t} P(\sigma,t) = \sum_{\sigma'} \Gamma(\sigma \mid \sigma') P(\sigma',t) , \tag{14}$$

the dynamic correlation functions can be represented in the spectral form as a superposition of exponential factors. Consider the eigenvectors and eigenvalues of the stochastic matrix Γ:

$$\sum_{\sigma'} \Gamma(\sigma \mid \sigma') \phi_\omega(\sigma') = -\omega \phi_\omega(\sigma) , \tag{15}$$

where $\omega \geq 0$. One can introduce the scalar product, which coincides with thermodynamic averaging, and orthonormalize the eigenvectors ϕ_ω. Straightforward eigenvector expansion gives then the following representation of the single-spin autocorrelation function,

$$\langle S_x(0) S_x(t) \rangle = \sum_\omega | \langle S_x \phi_\omega \rangle |^2 e^{-\omega t} . \tag{16}$$

It is more convenient and customary to use the correlation times $\tau = 1/\omega$, and to write, after configurational averaging

$$q(t) = \overline{\langle S_x(0) S_x(t) \rangle} = \int_0^\infty d\tau \rho(\tau) e^{-t/\tau} . \tag{17}$$

The weights $\rho(\tau)$ are interpreted here as the averaged correlation coefficients of individual spins with exponentially relaxing eigenvectors of Γ and are normalized by $\int d\tau \rho(\tau) = 1$.

For any finite system, as well as for some infinite systems, there will be a gap between the smallest eigenvalue ω_0 and 0. This would make it possible to define the longest relaxation time $\tau_{\max} = 1/\omega_0$, which is a direct analogue of the "true correlation range" of Ref. 35. The actual observation of asymptotic exponential decay, $\exp(-t/\tau_{\max})$, however, is possible only if the gap is sufficiently wide. Even for finite systems the appearance of nonexponential decay will result from dense clustering of eigenvalues close to $\omega = 0$. In such a situation one must deal with the entire distribution of correlation times $\rho(\tau)$ in order to characterize the dynamics of fluctuations. It is convenient to describe the distribution in terms of its moments, because they provide a direct link between theory and experiment. The moments have a simple representation

$$\int_0^\infty dy\, y^{k+1} \rho(y) = \frac{1}{k!} \int_0^\infty dt\, t^k q(t) \tag{18}$$

and also can be obtained from measurements of ac susceptibilities at low frequencies (see Sec. VIII), as well as from some other experiments. Normalization is not necessary in (18), since $q(0) = 1$.

The simplest characterization of the distribution $\rho(\tau)$ is the average correlation time

$$\tau_{\text{av}} = \int_0^\infty dy\, y \rho(y) = \int_0^\infty dt\, q(t) . \tag{19}$$

Although this formula gives more weight to shorter time scales than to long-time behavior, it is substantially less sensitive to noise in the data and to the choice of upper cutoff in numerical integration. It should be noted, however, that τ_{av} is not equal to the correlation time τ appearing in conventional scaling formulas. The dynamic scaling hypothesis,[34] valid for $T \to T_g$ and $t \gg 1$, can be written in the following form for the position-independent correlation function $q(t)$:

$$\begin{aligned} q(t) &\approx t^{-x} Q(t/\tau) , \\ x &= \frac{1}{2} \left[\frac{d-2+\eta}{z} \right] , \\ \tau &\approx (T - T_g)^{-z\nu} . \end{aligned} \tag{20}$$

Here z is the dynamic critical exponent. Note that I put a factor of $\frac{1}{2}$ in the definition of exponent x: this should be present because for spin glasses $q(t)$ plays the role of the order parameter rather than order-parameter correlation function appearing in Ref. 34; an analogous factor of $\frac{1}{2}$ can be seen in the case of simple ferromagnets when relax-

ation of magnetization, $\langle M(t)\rangle$, is compared to the magnetization correlation function, $\langle M(0)M(t)\rangle$.[36] Formula (20) is valuable, since it allows determination of the dynamic exponent z from algebraic decay of dynamic correlations close to the critical point.

Integration of the scaling form of the correlation function $q(t)$ (together with proper normalization of the scaling function) allows identification of the relevant correlation time

$$\tau=\int_0^\infty dt\, tq(t)\Big/\int_0^\infty dt\, q(t) = \int_0^\infty dy\, y^2\rho(y)\Big/\int_0^\infty dy\, y\rho(y)\ , \tag{21}$$

which is different from $\tau_{\rm av}$. Nevertheless, if dynamic scaling holds, one can determine the dynamic exponent z from $\tau_{\rm av}$ as well, since

$$\tau_{\rm av}=\text{const}\tau^{1-x} \tag{22}$$

with exponent x defined in (20), and const $=\int dy\, y^{-x}Q(y)$. This relation has not been recognized in earlier studies of spin glasses, and the exponent z quoted previously[15] should be more properly named $z_{\rm av}$, with

$$z_{\rm av}=z(1-x)=(2z-d+2-\eta)/2\ .$$

Differences between various definitions of the correlation time should also be remembered when scaling analysis of experimental data is performed.

Three complementary methods will be used here to determine the exponent z from correlation functions described in the preceding section.

(1) $\tau_{\rm av}(T)$ will be obtained from numerical integration of the data for $q(t)$ for use both in direct fitting and in finite-size-scaling analysis.

(2) Correlation time $\tau(T)$ defined in (21) as well as another estimate of $\tau_{\rm av}$ will be obtained from integration of the fitting function (13) for lattice size 64^3.

(3) Exponent x, defined in (20), will be determined from the power-law decay of $q(t)$ or $\chi_{\rm SG}(t)$ at $T=T_g$.

These three methods yield the estimates of exponent z in combination with static critical exponents which were quoted in sec. III, and therefore simultaneously provide another consistency test linking the static and dynamic critical behavior. The average correlation times $\tau_{\rm av}(T)$ for lattice size 64^3 computed by numerical integration of the data [with log-linear extrapolation for $T\le 1.40$, where value of $q(t)$ and the cutoff time would be larger than 10^{-2}] agree well with those computed by numerical integration of the fitting function (13).

For smaller lattice sizes finite-size effects at temperatures close to T_g exclude any direct fitting procedure, and only the values of $\tau_{\rm av}(T)$ obtained by numerical integration of data are considered. The correlation times $\tau(T)$ for size 64^3 have been obtained by numerical integration of the fitting function.

Power-law fits for $\tau_{\rm av}(T)$ and $\tau(T)$ are presented in Fig. 16. The value $T_g=1.175\pm0.025$ has been used for plotting. The error estimates for the exponents include the uncertainty of the estimate of T_g, this error rather than

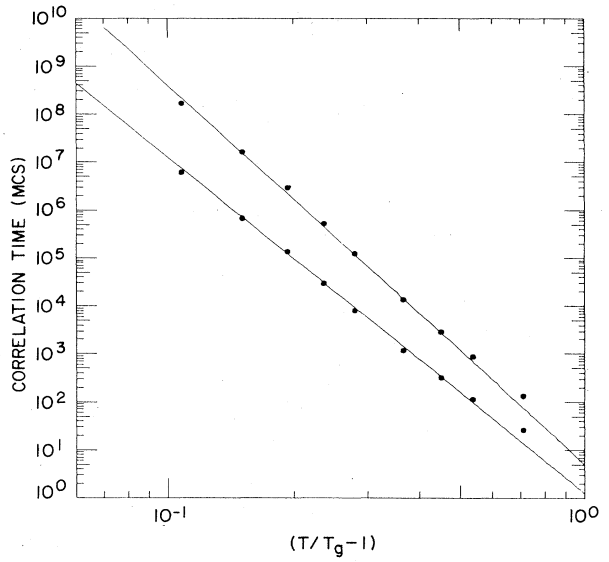

FIG. 16. Power-law fits $\tau=c(T-T_g)^{-z\nu}$ and $\tau_{\rm av}=c_{\rm av}(T-T_g)^{-z_{\rm av}\nu}$ for the relaxation times. Lattice size 64^3, $T\ge 1.30$.

scatter of the data is the major source of the magnitude of error bars. The fitting yields $z\nu=7.9\pm1.0$ and $z_{\rm av}\nu=7.0\pm0.8$, from which I get $z=6.1\pm0.3$ and $z_{\rm av}=5.4\pm0.2$.

Now I consider the average relaxation times for lattice sizes 8^3, 16^3, 32^3, and 64^3. The scaling function $\Theta(y)$, appearing in the finite-size dynamic scaling relation

$$\tau_{\rm av}(T)\approx L^{z_{\rm av}}\Theta[L^{1/\nu}(T-T_g)/T_g] \tag{23}$$

has been obtained. The minimal scatter of data points is achieved again by restricting T_g to the interval 1.15—1.20; with this uncertainty and the choice of $T_g=1.175\pm0.025$ I can align all data closest to a single curve by taking $\nu=1.3\pm0.1$ and $z_{\rm av}=5.4\pm0.4$, in good agreement with the value of $z_{\rm av}\nu$ determined by direct power-law fit to $\tau_{\rm av}(T)$ and with the estimate of ν from analogous finite-size-scaling analysis of nonlinear susceptibility, direct fitting of ξ as well as finite-size scaling of the so-called renormalized coupling constant.[25]

Exponents governing the algebraic decay of the order-parameter function $q(t)$ and its susceptibility $\chi_{\rm SG}(t)$ are shown in Fig. 17 for temperatures in the critical region and below T_g. Exponents for $\chi_{\rm SG}(t)$ are twice larger than for $q(t)$, as expected from scaling. Variation of $x(T)$ with temperature in the critical region above T_g seems to be linear to a very good approximation. Different temperature dependence is observed below T_g. From this plot we find

$$x(T_g)=(d-2+\eta)/2z=0.065\pm0.005\ .$$

Again, the error estimate results from uncertainty of the T_g estimate, and not from scatter of the data. The midpoint value $x(T_g)=0.065$ corresponds to $T_g=1.175$. The value of the dynamic exponent z obtained by this method is

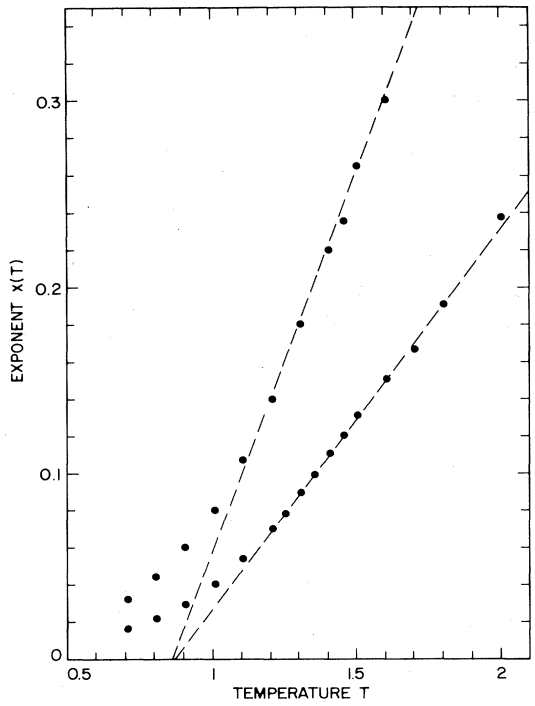

FIG. 17. Exponents $x(T)$ characterizing the algebraic decay of $q(t)$ (lower curve) and $\chi_{SG}(t)$. Exponents measured for nonlinear susceptibility are exactly twice larger than for $q(t)$ at each temperature. Straight lines are linear fits to the data in the critical region, a change of temperature dependence at T_g is well seen.

$$z=(7.7\pm0.5)(1+\eta)=6.0\pm0.8$$

when the estimate of $\eta=-0.22\pm0.05$ quoted earlier is used, and it agrees well with the number estimated from the analysis of relaxation times.

Different methods of analysis described in this section consistently support the view that the growth of correlation times as $T\to T_g$ is well described by critical slowing down, and distinct methods used to determine the dynamic exponents taken together yield the value of $z=6.0\pm0.8$, and $z_{av}=5.5\pm0.5$ or equivalently that the exponents which can be directly measured in experiments[6,37] are $z_{av}\nu=7.2\pm0.1$ and $z\nu=7.9\pm1$. Small differences between dynamic exponent estimates obtained from the decay of $q(t)$ at T_g on one hand and from correlation times *above* T_g on the other can be attributed to corrections to scaling, which are discussed in the next section.

VII. SCALING OF CORRELATION FUNCTIONS: CORRECTIONS TO SCALING

In view of the success of the dynamic scaling hypothesis in explaining the temperature dependence of correlation times, it is important to see if other predictions of dynamic scaling are also satisfied. The question is: Is the empirically found shape of the relaxation functions proposed in formula (13) consistent with the scaling law (20), if exponents $x(T)$ and $\beta(T)$ are temperature dependent, as shown in Figs. 11, 12, and 17? In order to reconcile the temperature dependence of the parameters with scaling, we remind the reader that, generally speaking, corrections to scaling should be included in (20), and one should have instead, for $T\to T_g$,

$$q(t)=t^{-x}Q(t/\tau)[1+t^{-x_1}Q_1(t/\tau)+\cdots]\ . \tag{24}$$

The first- and higher-order correction terms are expected to be responsible for the temperature dependence of parameters in the empirical formula for $q(t)$ found in Sec. V, which obviously is not written in the scaling form. Such a working hypothesis is more natural at this stage than an *ad hoc* assumption of some new anomalous dynamic scaling hypothesis, because conventional dynamic scaling[34] predictions worked well in explaining the relation between the dynamic exponent z characterizing the divergence of correlation times at T_g and the power-law decay of dynamic correlations. It should be said, however, that deviations from conventional dynamic scaling are not unthinkable for at least some random systems, and indeed have been proposed recently for dilute magnets at percolation threshold.[38]

Now, formula (24) is not useful for fitting the data when the form of functions Q, $Q_1,\ldots,$ and the exponents are not known *a priori;* an approximation to (24) obtained from Taylor expansions obviously contains so many free parameters that anything could be "explained." Therefore, in order to see if the observed temperature dependence of exponents $x(T),\beta(T)$ is consistent with corrections to scaling, I will proceed as follows. When T approaches T_g, long-time tails of $q(t)$ are strongly influenced by finite-size corrections and cannot be used in the scaling analysis which is appropriate for the infinite-volume limit. But short- and intermediate-time behavior is *not* affected by finite size for times $t\lesssim 10^4$ MCS already for lattices of size 16^3 and 32^3.

Therefore, the predictions of the conventional dynamic scaling hypothesis that might apply to these time scales can be verified, especially if not too many free parameters need to be introduced. I have looked at the variation of $q(t)$ with temperature at fixed time t, since it is reasonable to assume that if dynamic scaling holds, one should have the expansion

$$q(t;T)=q(t;T_g)-a_1(T-T_g)^{\Delta_1,\delta_1}+\cdots\ . \tag{25}$$

Here one compares the value of the function $q(t)$ at temperature T above T_g with the value of $q(t)$ exactly at T_g at fixed time. The correction exponents Δ_1,δ_1 and the amplitude a_1 are, of course, independent of temperature.

In order to verify if formula (25) holds, I have examined the data in four decades of time: $t=10$, 96, 1024, and 10240 MCS, and for temperatures in the range $1.20\le T\le 1.50$, which is quite generous as the dynamic critical regime need not extend so far from T_g, which will be taken to be $T_g=1.20$ in this analysis. I have plotted the differences $q(t;T_g)-q(t;T)$ as functions of t and $T-T_g$ in order to test the hypothesis (25), viz. to see if

$$\ln[q(t;T_g)-q(t;T)]\approx u(t)+\Delta_1\ln(T-T_g)\ ,$$

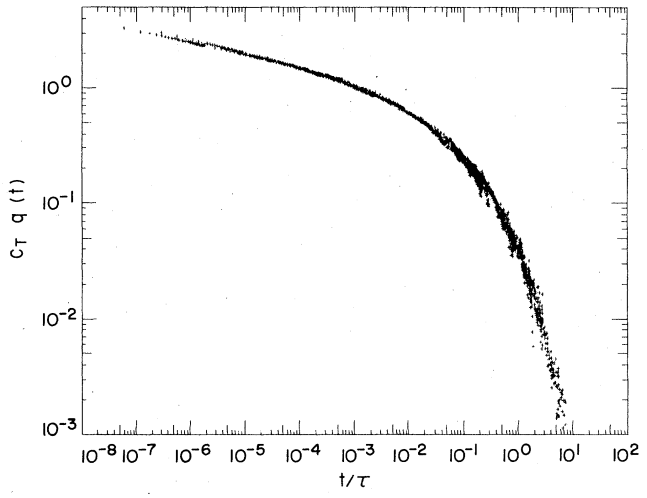

FIG. 18. Dynamic correlation functions $q(t)$ from Fig. 7 are plotted here in the scaling form $c\cdot q(t)\approx Q(t/\tau)$. Parameters c are obtained by matching the correlation functions so that minimal scatter of points is obtained. Values of correlation times $\tau(T)$ were determined as described in Sec. VI.

with $u(t)=\ln a_1+\delta_1 \ln t$. First, for each value of time t the data were plotted in the above form as functions of $\ln(T-T_g)$ in order to see if straight lines are obtained, and the slope Δ_1 is the same for all times. Then I plotted the intercepts $u(t)$ versus $\ln t$; they should lie on a straight line with slope δ_1.

I have found that even for this wide range of temperatures ($T_g < T \leq 1.50$) the strong scaling prediction (25) is satisfied quite nicely for times $t \lesssim 10^3$, while for longer times systematic deviations get progressively larger at higher temperatures. One would need higher-order corrections in (25) to describe longer time scales and higher temperatures. The fitted values of parameters are also reasonable: $a \approx 2.65$, $\Delta_1 \approx 1.1$, and $\delta_1 \approx 0.17$.

In conclusion I would say that the shape of relaxation functions $q(t)$ determined in this work is consistent with conventional dynamic scaling hypothesis if one allows for non-negligible corrections in the scaling formula (24). In fact the data shown in Fig. 7 can be plotted in the scaling form (Fig. 18), but systematic deviation of data from what should be a single curve are clearly seen at closer inspection.

VIII. EXPERIMENTAL SITUATION

In this section I will outline the relation of the present work to experimental characterization of the dynamics of spin glasses. One should keep in mind that samples used in experiments may not satisfy the symmetry condition (5) (which is important for comparison of results) due to chemical clustering and residual short-range magnetic order. This feature complicates the interpretation of experimental data. Here I will assume a working hypothesis that strongly cooperative phenomena and scaling observed in the vicinity of spin-glass transition are not distorted too much by possible effects of short-range clustering.

Fluctuations at temperatures close to T_g involve long-time scales, and are well probed by low-frequency ac susceptibility measurements. The simplest, and most commonly used experimental measure of a "characteristic time" $\bar{\tau}$ which is some sense describes the dynamic range of fluctuations is obtained from the temperature $T_f(\nu)$ at which in-phase linear susceptibility $\chi'(\nu)$ reaches a maximum at fixed frequency ν by a relation $\bar{\tau}(T_f)\approx\nu^{-1}$. Attempts were made[7] to estimate the dynamic exponent from the formula

$$\bar{\tau}(T_f)\approx\tau_0(1-T_g/T_f)^{-z\nu} . \tag{26}$$

The trouble with formula (26) is that it is only a rather crude approximation (even for exponentially relaxing systems) to any definition of correlation time based on moments of dynamic correlation functions, and thus it is not very useful for comparison with theoretical predictions. I expect that (26) can give only some feeling about the magnitude of dynamic exponents which are defined by the scaling relations. In contrast to (26), ac measurements can be analyzed in a more sophisticated way to determine directly the dynamic critical exponent. A method recently used[6] begins with standard relations ($\omega=2\pi\nu$)

$$\chi'(\omega)=\chi_T\int d\tau\rho(\tau)\frac{1}{1+\omega^2\tau^2} ,$$
$$\chi''(\omega)=\chi_T\int d\tau\rho(\tau)\frac{\omega\tau}{1+\omega^2\tau^2} . \tag{27}$$

In the limit of small frequencies one obtains

$$\lim_{\omega\to 0}\frac{1}{\omega}\frac{\chi''(\omega)}{\chi'(\omega)}=\int d\tau\,\tau\rho(\tau)=\tau_{\rm av} . \tag{28}$$

This is the average correlation time, and definition (28) coincides with formula (19) if condition (5) is (approximately) satisfied. The estimate of $z_{\rm av}\nu$ measured in the $En_{0.4}Sr_{0.6}S$ sample[6] is $z_{\rm av}\nu=7.2\pm0.5$, which is in agreement with the number 7.2 ± 1 obtained in Monte Carlo simulations. Very recently the same method has been used in the experiment with Mn aluminosilicate spin glass,[37] and the value of $z_{\rm av}\nu=7.6\pm0.2$ has been obtained from the best fit. In both cases it has been found in addition that scaling laws for $\tau_{\rm av}(T,H)$ are well satisfied.

It is interesting to note that also the correlation time τ introduced in Eq. (21) could be obtained from these measurements, if one uses another formula

$$\lim_{\omega\to 0}\frac{1}{\omega}\frac{\chi_T-\chi'(\omega)}{\chi''(\omega)}=\tau \tag{29}$$

which is obtained from (27) in an analogous manner. It would be very interesting to analyze experimental data using both methods; in fact Eq. (29) which [unlike (28)] includes terms of order $(\omega\tau)^2$ in the expansion can be more accurate at small, but finite frequencies.

At present experiments do not permit a good determination of the shape of the dynamic correlation function $q(t)$. At least in principle, however, if the structure factor $S(q,\omega)$ is approximately independent of q one could cover a fantastic range of times scales from 10^{-12} to about 1 sec by combining the neutron spin echo, muon spin relaxa-

tion, and ac susceptibility measurements. Existing compilation of data for CuMn spin glass[39] shows that decay is certainly not exponential even at short times above T_g, and that below T_g the correlation function does not appear to decay to a constant even at times of order 10^{-2} sec. More experimental data on the shape of correlation functions would be most interesting.

IX. SUMMARY

I have presented the description of the dynamics of equilibrium fluctuations in Ising spin glasses. For the first time the analysis was performed in a wide range of time scales, and for both high and low temperatures, in large-scale Monte Carlo simulations. The computation took over half a year of time on the special purpose computer, which was necessary to probe the long-time behavior and to reduce statistical errors. This amount of computing can be roughly compared to several years of the Cray-1 time. The results are encouraging, and the simple-model Hamiltonian (1) appears to have a similar relation to at least some real spin glasses as the ordinary Ising model has to real nonrandom magnetic materials.

The main results can be summarized as follows.

(1) Decay of dynamic correlations is nonexponential below the Curie point of the nonrandom Ising model. Above $T_g=1.175\pm0.025$ the empirical formula $q(t)=ct^{-x}\exp[-\omega t^{\beta}]$, with temperature-dependent exponents x and β, provides an excellent fit to the data both at short and long times. The power-law decay stretches to ever longer times as the temperature approaches T_g. Below T_g only power-law decay could be observed at all time scales which are not influenced by finite-size effects, and the temperature dependence of exponent $x(T)$ was found to be different from that seen above T_g. Nonexponential decay can be formally described by a distribution of correlation times $\rho(\tau)$, and it has been proposed that in this system the asymptotic Kohlrausch function results from averaging over approximately uncorrelated contributions of localized fluctuations which are due to local variations of the density of frustration in an inhomogeneous lattice. A model of independent rigid clusters does not provide the appropriate description of these processes.

(2) The correlation times diverge rapidly when temperature approaches T_g from above. The divergence is well described by a power law $\tau\approx\tau_0(T/T_g-1)^{-z\nu}$, with $z\nu=7.9\pm1$ for a correlation time defined as the normalized second moment of $\rho(\tau)$. The average correlation time diverges with the exponent $z_{\rm av}\nu=7.2\pm1$. The dynamic scaling hypothesis establishes the scaling laws involving these two and other exponents, and I find that these relations are indeed satisfied when separately computed static critical exponents are substituted.

(3) The dynamic correlation function does not scale in a simple way. One can argue that this is due to corrections to scaling, and while conventional dynamic scaling indeed appears to be sufficient to explain the data, a possibility that a modified scaling law should be used for random systems like spin glasses cannot be excluded.

(4) The magnitude of critical exponents, and the rather unusual behavior of the spin-glass phase below T_g are not typical for a simple phase transition to a state with long-range order. This suggests that $d=3$ is either a marginal dimension, or close to it. So far, scaling arguments involving a rather narrow range of temperatures below T_g and lattice sizes $L\leq16$ are consistent with the hypothesis that the spin-glass phase is always critical at all $T\leq T_g$, i.e., that there is no true long-range order but rather that static and dynamic correlations decay algebraically. An earlier study showed that static correlation functions appear to decay to a constant below T_g. This could be an effect of periodic boundary conditions, or of inadequate number of samples used for configurational averaging. On the other hand, the apparent critical behavior at $T<T_g$ could equally well result from peculiar finite-size effects, not unlike those seen in one-dimensional spin glasses with long-range interactions.[40] So far, the issue of the nature of the spin-glass phase has not been completely resolved. Further work, both conceptual and numerical, is needed to clarify this point.

(5) Dynamic critical exponent $z_{\rm av}\nu=7.2\pm1$ is quite close to the experimental value of about 7.0—7.5 recently measured for two insulating spin glasses with short-range exchange interactions. Let sophisticated experimental estimates of the dynamic exponent for metallic spin glasses give smaller values. The static critical exponents obtained from numerical simulations, in particular the nonlinear susceptibility exponent $\gamma\approx3$ and specific-heat exponent $\alpha\approx-2$ are also quite sensible when compared with existing experimental data. Further experimental work, at lower frequencies and with higher precision, would be very desirable.

ACKNOWLEDGMENTS

Numerous useful discussions with D. Huse and C. Henley are gratefully acknowledged. I have also benefitted from conversations with P. Hohenberg, D. S. Fisher, P. W. Anderson, and R. N. Bhatt.

[1] B. R. Coles, in *Multicritical Phenomena,* edited by R. Pynn and A. Skjeltorp (Plenum, New York, 1984), p. 363.

[2] A review of recent work and an extensive list of references can be found in C. Y. Huang, J. Magn. Magn. Mater. (to be published).

[3] A. P. Murani, J. Magn. Magn. Mater. **22**, 271 (1981), **31-34**, 1327 (1983).

[4] F. Mezei, J. Appl. Phys. **53**, 7654 (1982).

[5] D. Hüser, L. E. Wenger, A. J. van Duyneveldt, and J. A. Mydosh, Phys. Rev. B **27**, 3100 (1983).

[6] N. Bontemps, J. Rajchenbach, R. V. Chamberlin, and R. Orbach, Phys. Rev. B **30**, 6514 (1984).

[7] J. Souletie and J. L. Tholence, Phys. Rev. B **32**, 516 (1985).

[8] Scott Kirkpatrick and David Sherrington, Phys. Rev. B **17**, 4384 (1978).

[9] H. Sompolinsky and Anette Zippelius, Phys. Rev. Lett. **47**, 359 (1981); Phys. Rev. B **25**, 6860 (1982).

[10] W. L. McMillan, J. Phys. C **17**, 3179 (1984).

[11]W. L. McMillan, Phys. Rev. B **28**, 5216 (1983).
[12]J. D. Reger and A. Zippelius (unpublished).
[13]A. P. Young, Phys. Rev. Lett. **50**, 9171 (1983).
[14]David A. Huse and I. Morgenstern, Phys. Rev. B **32**, 3032 (1985).
[15]Andrew T. Ogielski and Ingo Morgenstern, Phys. Rev. Lett. **54**, 928 (1985); J. Appl. Phys. **57**, 3382 (1985).
[16]K. Binder and A. P. Young, Phys. Rev. B **29**, 2864 (1984).
[17]J. L. Tholence, Solid State Commun. **35**, 113 (1980).
[18]H. Vogel, Phys. Z. **22**, 645 (1921); G. S. Fulcher, J. Am. Ceram. Soc. **8**, 339 (1925).
[19]L. Lundgren, P. Svedlinh, and O. Beckman, Phys. Rev. B **26**, 3990 (1982).
[20]Deepak Dhar, in *Stochastic Processes, Formalism and Applications,* Vol. 184 of *Lecture Notes in Physics* (Springer, Berlin, 1983), p. 300.
[21]Mohit Randeria, James P. Sethna, and Richard G. Palmer, Phys. Rev. Lett. **54**, 1321 (1985).
[22]R. G. Palmer, D. L. Stein, E. Abrahams, and P. W. Anderson, Phys. Rev. Lett. **53**, 958 (1984).
[23]S. F. Edwards and P. W. Anderson, J. Phys. F **5**, 965 (1975).
[24]G. Toulouse, Commun. Phys. **2**, 115 (1977); P. W. Anderson, J. Less-Common Met. **62**, 291 (1978).
[25]R. N. Bhatt and A. P. Young, Phys. Rev. Lett. **54**, 924 (1985).
[26]F. Mezei, J. Appl. Phys. **53**, 7654 (1982).
[27]M. Mézard, G. Parisi, N. Sourlas, G. Toulouse, and M. Virasoro, Phys. Rev. Lett. **52**, 1156 (1984).
[28]C. E. Shannon and W. Weaver, *Mathematical Theory of Communication* (Urbana University Press, Urbana, 1949).
[29]A. P. Young, J. Phys. C **18**, L517 (1984).
[30]Andrew T. Ogielski, Bull. Am. Phys. Soc. **30**, 624 (1985).
[31]Andrew T. Ogielski (unpublished).
[32]Robert B. Griffiths, Phys. Rev. Lett. **23**, 17 (1969).
[33]J. H. Condon and A. T. Ogielski, Rev. Sci. Instrum. **56**, 1691 (1985).
[34]P. C. Hohenberg and B. I. Halperin, Rev. Mod. Phys. **49**, 435 (1977).
[35]Michael E. Fisher and Robert J. Burford, Phys. Rev. **156**, 583 (1967).
[36]Masuo Suzuki, Progr. Theor. Phys. **58**, 1142 (1977).
[37]J. A. Hamida and S. J. Williamson (private communication). I thank them for communicating the results prior to publication. The quoted value of $z_{av}\nu$ corresponds to $T_g = 2.95 \pm 0.02$ for this sample.
[38]C. Henley, Phys. Rev. Lett. **54**, 2030 (1985).
[39]Y. J. Uemura, D. R. Harshman, M. Senba, E. J. Ansaldo, and A. P. Murani, Phys. Rev. B **30**, 1606 (1984).
[40]R. N. Bhatt and A. P. Young, J. Appl. Phys. (to be published).